SYNCHRONIZATION OF CHAOS IN PHASE-LOCKED LOOPS

by

Tetsuro Endo and Leon O. Chua

Memorandum No. UCB/ERL M91/59

1 May 1991

SYNCHRONIZATION OF CHAOS IN PHASE-LOCKED LOOPS

by

Tetsuro Endo and Leon O. Chua

Memorandum No. UCB/ERL M91/59

1 May 1991

ELECTRONICS RESEARCH LABORATORY

College of Engineering
University of California, Berkeley
94720

TITLE PAGE

This research was supported in part by the National Science Foundation grant MIP-8912639 and the Office of Naval Research grant N00014-89-J-1402.

SYNCHRONIZATION OF CHAOS IN PHASE-LOCKED LOOPS

by

Tetsuro Endo and Leon O. Chua

Memorandum No. UCB/ERL M91/59

1 May 1991

ELECTRONICS RESEARCH LABORATORY

College of Engineering
University of California, Berkeley
94720

This research was supported in part by the National Science Foundation grant MIP-8912639 and the Office of Naval Research grant N00014-89-J-1402.

Synchronization of Chaos in Phase-Locked Loops

Tetsuro Endo[†], member and Leon O. Chua, fellow[††]

[†] Department of Electrical Engineering, The National Defense Academy, 1-10-20 Hashirimizu, Yokosuka 239 Japan

[††] Department of Electrical Engineering and Computer Sciences, University of California, Berkeley CA94720 U.S.A.

Abstract-This note presents the first experimental demonstration that two *phase-locked loops* driven by a common *chaotic* signal derived from a master phase-locked loop can be *synchronized* under some suitably chosen but robust range of system parameters. Experimental observations are completely consistent with both computer simulations, and with the recent synchronization criterion due to Pecora and Carrol. The robustness of this synchronization scheme suggests the intriguing possibility of achieving *secure* communication through chaos.

1. Introduction

Chaos is believed to defy synchronization. Namely, two identical chaotic systems started at nearly the same initial points in phase space have trajectories which quickly become uncorrelated, even though each system traces the same attractor in phase space. Recently, Pecora and Carroll reported that a sub-system of a chaotic system could be synchronized with a separate chaotic system under certain conditions [1][2]. Synchronization in chaotic systems seems to be an interesting problem not only from a purely theoretical viewpoint but also from a practical engineering viewpoint. Indeed, if chaos can be synchronized, it could give rise to new applications, such as using chaos for secure communications.

Previously, we reported that the phase of the voltage controlled oscillator (VCO) of phase-locked loops (PLL's) can become chaotic under certain conditions [3][4]. We now investigate whether or not a PLL can be synchronized with this chaotically modulated VCO signal. We have discovered a very interesting phenomenon whereby the chaotic VCO outputs of two almost identical PLL's can be synchronized in a certain circuit configuration. Namely, two identical PLL's driven by a common chaotically modulated input signal (therefore, the VCO outputs are also chaotic) can achieve a one-to-one synchronization (configuration 1). In contrast, the chaotic VCO outputs of two almost identical PLL's driven by a common frequency modulated signal with detuning, cannot be synchronized (configuration 2). In this paper, we report some experimental observations and the associated computer simulations concerning the synchronization of chaos in the two systems of PLL's shown in Figs. 1 and 2. We also investigate theoretically the conditions for synchronization and non-synchronization of chaos in PLL's. In particular, we found that the sub-system receiving a chaotic driving signal from the master system can synchronize only if the Lyapunov exponents of the sub-system are all negative. By calculating these Lyapunov exponents, we verify that they are all negative in configuration 1, while one of them is positive in configuration 2. These results are completely consistent with our experiments and computer simulations.

2. DERIVATION OF DIFFERENTIAL EQUATIONS FOR CONFIGURATION 1 AND CONFIGURATION 2

In this section, we will derive the differential equations governing configuration 1 and configuration 2. We derive first the differential equation for configuration 1 which consists of two almost identical PLL's receiving a common chaotic input signal generated from another PLL. The theory, experiments and the associated computer simulations of chaos generated in PLL's are reported in our previous papers [3]-[5]. Here we investigate the PLL system shown in Fig.1 consisting of three PLL's, where the PLL0 is used for generating chaos, and where its chaotic VCO output is applied to the input of both PLL1 and PLL2 which are almost identical. Here we will assume the following properties for all PLL's.

1) The loop filter is assumed to be a lag filter of the form:

$F_0(s)=1/(1+\tau_0 s)$, $F_1(s)=1/(1+\tau_1 s)$, $F_2(s)=1/(1+\tau_2 s)$.

2) The VCO free-running frequencies of PLL0 and PLL1 are equal, but there exists a frequency detuning $\Delta\omega_{vco}$ between PLL0 and PLL2.

From Fig.1 the differential equation of the phase error ϕ_0 can be calculated as follow:

$$d^2\phi_0/dt^2 + (1/\tau_0)d\phi_0/dt + (K_0/\tau_0)h(\phi_0) = d^2\theta_i/dt^2 + (1/\tau_0)d\theta_i/dt \quad (1a)$$

where

$$d\theta_i/dt = \Delta\omega + M \sin \omega_m t \quad (1b)$$

and where $\Delta\omega$ is the detuning between the carrier frequency and the VCO free-running frequency of the PLL0, M is the maximum angular frequency deviation, ω_m is the angular frequency of modulation. In the same manner, the differential equation of the phase errors ϕ_1 and ϕ_2 can be written respectively as follow:

$$d^2\phi_1/dt^2 + (1/\tau_1)d\phi_1/dt + (K_0/\tau_1)h(\phi_1) = d^2\theta_{in}/dt^2 + (1/\tau_1)d\theta_{in}/dt \quad (2)$$

$$d^2\phi_2/dt^2 + (1/\tau_2)d\phi_2/dt + (K_0/\tau_2)h(\phi_2) = d^2\theta_{in}/dt^2 + (1/\tau_1)d\theta_{in}/dt \quad (3)$$

where

$$\theta_{in}(t) = \theta_0{}^0(t) = \theta_i(t) - \phi_0(t) . \quad (4)$$

By changing the time variable t into t' via $t'=\omega_n t$ and defining the state variables $x_1=\phi_0$, $x_2=d\phi_0/dt'$, $x_3=\phi_1$, $x_4=d\phi_1/dt'$, $x_5=\phi_2$, and $x_6=d\phi_2/dt'$, equations (1) to (4) can be recast into the following *6th-order* system of non-autonomous differential equations:

$$dx_1/dt' = x_2$$

$$dx_2/dt' = -\beta x_2-h(x_1)+\beta\sigma+m\beta \sin\Omega t' +m\Omega \cos\Omega t'$$

$$dx_3/dt' = x_4$$

$$dx_4/dt' = -\kappa_1\beta x_4 - \kappa_1 h(x_3)+h(x_1)+\beta(\kappa_1-1)(-x_2+\sigma+m \sin\Omega t')$$

$$dx_5/dt' = x_6$$

$$dx_6/dt'= -\kappa_2\beta x_6-\kappa_2 h(x_5)+h(x_1)+\beta(\kappa_2-1)(-x_2+\sigma+m \sin\Omega t')+\beta\kappa_2\delta \qquad (5)$$

where $\omega_n=\sqrt{K_0/\tau_0}$ (natural angular frequency), $\beta=\omega_n/K_0=1/\sqrt{K_0\tau_0}$ (normalized natural angular frequency), $\kappa_1=\tau_0/\tau_1$ (ratio of the loop filter time constants), $\kappa_2=\tau_0/\tau_2$ (ratio of the loop filter time constants), $\sigma=\Delta\omega/\omega_n$ (normalized frequency detuning of the input FM carrier frequency), $m=M/\omega_n$ (normalized maximum angular frequency deviation), $\Omega=\omega_m/\omega_n$ (normalized modulation frequency) and $\delta=\Delta\omega_{vco}/\omega_n$ (normalized frequency detuning of the PLL2).

Let us investigate next the second system consisting of two almost identical PLL1 and PLL2 having a common input consisting of a frequency modulated sinusoid with detuning. We call this system configuration 2 and is shown in Fig.2. Assuming the same lag filter for $F_1(s)$ and $F_2(s)$ as before, the differential equations of the phase errors ϕ_1 and ϕ_2 can be written as follow:

$$d^2\phi_1/dt^2 + (1/\tau_1)d\phi_1/dt + (K_0/\tau_1)h(\phi_1) = d^2\theta_i/dt^2 + (1/\tau_1)d\theta_i/dt \qquad (6)$$

and

$$d^2\phi_2/dt^2 + (1/\tau_2)d\phi_2/dt + (K_0/\tau_2)h(\phi_2) = d^2\theta_i/dt^2 + (1/\tau_2)d\theta_i/dt \qquad (7)$$

where

$$d\theta_i/dt = \Delta\omega + M \sin \omega_m t\,. \qquad (1b)$$

Applying the similar normalizations as in configuration 1 (e.g.; $t'=\omega_n t$, $\omega_n=\sqrt{K_0/\tau_1}$) and defining the state variables $x_1=\phi_1$, $x_2=d\phi_1/dt'$, $x_3=\phi_2$, and $x_4=d\phi_2/dt'$, this system can be recast into the following *4th-order* system of non-autonomous differential equations:

$$\begin{aligned}
dx_1/dt' &= x_2\\
dx_2/dt' &= -\beta x_2-h(x_1)+m\Omega\cos\Omega t'+\beta\sigma+m\beta\sin\Omega t'\\
dx_3/dt' &= x_4\\
dx_4/dt' &= -\kappa_1\beta x_4-\kappa_1 h(x_3)+m\Omega\cos\Omega t'+\kappa_1\beta\sigma+\kappa_1\beta m\sin\Omega t'
\end{aligned} \qquad (8)$$

where $\beta= \omega_n /K_0=1/\sqrt{K_0\tau_1}$, $\kappa_1=\tau_1/\tau_2$.

3. COMPUTER SIMULATION RESULTS

In this section we will present our computer simulation results for both configuration 1 (eq.(5)) and configuration 2 (eq.(8)). We present first our computer simulation results of configuration 1, as represented by eq.(5) for the small damping case with $\zeta=0.28$, β $(=2\zeta) = 0.56$, $\sigma=1.43341$, and $\Omega=0.637$. The initial conditions are $x_1(0)=2.3389$ and $x_2(0)=2.8027$ for the PLL0, $x_3(0)=0.1$ and $x_4(0)=0.1$ for the PLL1, and $x_5(0)=0.09$ and $x_6(0)=0.09$ for the PLL2.

Note that there is a 10 % difference between the initial conditions for the PLL1 and the PLL2. It is known that the VCO output of the PLL0 is chaotic for the above choice of parameter values [4]. Our goal is to investigate the dynamical behavior of the VCO outputs of PLL1 and PLL2 when their common input, i.e., the VCO output of the PLL0, is chaotic. In particular, we investigate whether or not PLL1 and PLL2 can synchronize with each other over some range of system parameter values. In particular, we assume 5 slightly different sets of parameter values for PLL1 and PLL2.

Figure 3 presents the simplest situation in which PLL0, PLL1 and PLL2 have the same loop filter time constants (κ_1=1 and κ_2=1) and the same VCO free-running frequencies (δ=0); i.e., the three PLL's have the same system parameter values. Figure 3(a) shows a Poincare section of the attractor of the state variables x_1 and x_2 (ϕ_0 versus $d\phi_0/dt'$) taken at every period $T=2\pi/\Omega$ of the external force. Observe that the VCO output of the PLL0 is indeed chaotic. Fig.3(b) shows the attractor in the x_3 versus x_4 (ϕ_1 versus $d\phi_1/dt'$) plane thereby confirming that the internal dynamics of the PLL1 is chaotic. Fig.3(d) shows the attractor in the x_5 versus x_6 (ϕ_2 versus $d\phi_2/dt'$) plane. Observe that the PLL2 is also chaotic and exhibits the same attractor as PLL1. Figure 3(c) shows a trace on Poincare section relating the two chaotic state variables x_3 and x_5 (ϕ_1 versus ϕ_2). Observe that there is an exact one-to-one (i.e., complete) synchronization between the two phase errors ϕ_1 and ϕ_2 in spite of the 10 % difference in the initial conditions of the PLL1 and the PLL2.

Figure 4 presents the attractors corresponding to those in Fig.3 but for the case where the loop filter time constants of the PLL1 and the PLL2 differ by 5 % of that of the PLL0 (κ_1=1.05 and κ_2=0.95) and where there is no detuning of the VCO free-running frequencies (δ=0). Observe that although the chaotic attractors shown in Figs.4(b) and (d) differ to some extent in this case, there remains a strong partial correlation between x_3 and x_5 (ϕ_1 and ϕ_2) in Fig.4(c).

Figure 5 shows three Poincare sections relating x_3 and x_5 (ϕ_1 versus ϕ_2) for the following 3 *distinct* sets of parameter values: (a) κ_1=1.0, κ_2=1.0 and δ=0.01 (equal loop filter time constants with small detuning), (b) κ_1=1.01, κ_2=0.99 and δ=0.0 (unequal loop filter time constants with no detuning), (c) κ_1=1.0, κ_2=1.0 and δ=0.1 (equal loop filter time constants with large detuning). The strong correlation exhibited by these three examples suggests that the synchronization is quite robust.

Consider next our computer simulations of eq.(5) for the case where the damping is large. In particular, we choose ζ=0.635, β (=2ζ)=1.27, σ=1.15, Ω=0.2; with the initial condition $x_1(0)$=1.6811 and $x_2(0)$=3.4605 for the PLL0, $x_3(0)$=0.1 and $x_4(0)$=0.1 for the PLL1, and $x_5(0)$=0.09 and $x_6(0)$=0.09 for the PLL2. Figure 6 presents the case with equal loop filter (κ_1=1, κ_2=1) and with no detuning (δ=0). Figure 6(a) shows the chaotic attractor of the PLL0 in the x_1 versus x_2 (ϕ_0 versus $d\phi_0/dt'$) plane. Recall that the output of this chaotic system is the *common* chaotic input signal for both PLL1 and PLL2. Figures 6(b) and (d) show the attractors in the x_3 versus x_4 (ϕ_1 versus $d\phi_1/dt'$) plane and in the x_5 and x_6 (ϕ_2 versus $d\phi_2/dt'$) plane. Observe that they are virtually identical. Figure 6(c) confirms that there is an exact one-to-one synchronization between PLL1 and PLL2. If we introduce some detuning (δ=0.05) without changing other parameters, we obtain the corresponding results shown in Fig.7. Observe that some synchronization still exists. Figures 8(a), (b), and (c) are traces of the Poincare section on the x_3 versus x_5 (ϕ_1 versus ϕ_2) plane for 3 different sets of parameters showing that the synchronization is also quite robust for the large damping case: (a) κ_1=1.05, κ_2=0.95, δ=0 (unequal loop filter time constants and no detuning); (b) κ_1=1.1, κ_2=0.9, δ=0 (unequal loop filter time constants and no detuning); (c) κ_1=1.0, κ_2=1.0, δ=0.1 (equal loop filter time constants with large detuning). Observe that Figs.8(a) and (b) show complete synchronization, as expected, while Fig.8(c) shows no synchronization because the PLL2 is out-of-lock itself, let alone synchronizing with the PLL1.

Next, we will present computer simulation results of configuration 2 (eq.(8)). Fig.9 shows the attractors on the Poincare section for the small damping case (ζ=0.28, β (=2ζ)=0.56, σ=1.43341, Ω=0.637, m=0.097) with the initial condition $x_1(0)$=2.3389 and $x_2(0)$=1.8027 for the PLL1 and a slightly different initial condition $x_3(0)$=2.3365 and $x_4(0)$=1.8009 for the PLL2. Note that these two sets of initial conditions have only a 0.1 % difference. Figure 9(a) is a chaotic attractor for the PLL1 observed in the x_1 versus x_2 plane, while Fig.9(b) is an identical chaotic attractor for the PLL2 observed in the x_3 versus x_4 plane. Observe that the trace between x_1 and x_3 in Fig.9(c) reveals no correlation whatsoever, which means that the PLL1 and the PLL2 cannot be synchronized with each other even if their system parameters are identical, thereby exhibiting identical attractors. We have also repeated our simulation for the large damping case (ζ=0.635, β(=2ζ)=1.27, σ=1.15, Ω=0.2, m=0.054) with the initial condition $x_1(0)$=1.6811 and $x_2(0)$=2.4605 for the PLL1, and with a slightly different initial condition $x_3(0)$=1.6794 and $x_4(0)$=2.4580 for the PLL2. The difference between the two sets of initial conditions is only 0.1 % as before. Again, Figs.10 (a), (b) and (c) show that there is no synchronization between PLL1 and PLL2 in configuration 2 for the large damping case, although they have completely the same attractors.

These results of our computer simulations can be summarized as follow:

For configuration 1:

1) Synchronization of chaos between the PLL1 and the PLL2 is possible for both the small and the large damping cases with the same system parameters ($\kappa_1=\kappa_2=1$ and $\delta=0$) but with a 10 % difference in their respective initial conditions. Moreover, this synchronization continues to hold even for a certain

amount of system parameter variations (κ_1, κ_2 = 0.9~1.1 and δ=0~0.1). Such robustness suggests that synchronization of chaos is possible in real systems.

2) The degradation of synchronization due to a mismatch of loop-filter time constants is more serious in the small damping case than in the large damping case. In contrast, the degradation due to the detuning of the VCO free-running frequencies is more serious in the large damping case than in the small damping case.

For configuration 2:

3) Synchronization of chaos in configuration 2 is impossible for both the small and the large damping cases,even for the same choice of system parameters; e.g., κ_1, κ_2 = 1 and δ=0. If there is some discrepancy of parameter values, synchronization of chaos is, of course, also impossible. In configuration 2, a very small difference in the initial conditions and /or parameter values of the PLL1 and the PLL2 gives rise to complete asynchronization.

4. CALCULATION OF SUB-SYSTEM LYAPUNOV EXPONENTS

In this section, we will apply the results of Pecora and Carrol [1][2] to explain why synchronization of chaos is possible in configuration 1 but not in configuration 2. Let us consider the n-dimensional dynamical system defined by dv/dt=g(v,w), dw/dt=h(v,w), and dw'/dt=h(v,w') where $v \in R^m$, $w,w' \in R^{n-m}$, $g:R^m \times R^{n-m} \rightarrow R^m$, and $h:R^m \times R^{n-m} \rightarrow R^{n-m}$. In this dynamical system, the v-w sub-system is called the drive system, since it runs independently of w' and the v signal is used to drive the w' subsystem. Consequently, we call the w' sub-system the response system. Under the right condition, and as time elapses, the w'(t) variables will converge asymptotically to the w(t) variables and continue to remain in step with the instantaneous values of w(t). The necessary and sufficient conditions for this to happen are determined by the signs of the "v-constrained" Lyapunov exponents of the w sub-system. They are calculated from the variational system *with respect to* w: $d\xi/dt=D_w h(v(t),w(t))\xi$ where

$D_w h$ is the Jacobian of the w sub-system with respect to w only. If all Lyapunov exponents of the variational equation are negative, w(t) and w'(t) will synchronize eventually. If at least one of them is positive, they will not synchronize.

For configuration 1, represented by equation (5), the set of state variables (x_1,x_2,x_7) can be identified with $v \in R^3$, (x_3,x_4) can be identified with $w \in R^2$ and (x_5,x_6) can be identified with $w' \in R^2$, where $x_7 \equiv \Omega t'$ has been introduced in order to convert our nonautonomous system into an autonomous system. The variational equation of (5) with respect to w becomes:

$$
\begin{aligned}
d\xi_1/dt' &= \xi_2 \\
d\xi_2/dt' &= -\kappa_1 h'(x_3)\xi_1 - \kappa_1 \beta \xi_2 \qquad (9)
\end{aligned}
$$

Thus solving (5) and (9) as a system of differential equations, we can calculate the Lyapunov exponents for configuration 1.

For example, we have calculated the Lyapunov exponents for the w sub-system for the small damping case shown in Fig.3 to be LE1=-0.241<0 and LE2=-0.319<0. Hence synchronization occurs even for a chaotic input signal generated by the PLL0, whose Lyapunov exponents have been calculated to be LE1=0.0296>0, LE2=0.00438≈0 and LE3=-0.594<0. Similarly, we have calculated the Lyapunov exponents of the w sub-system for the large damping case shown in Fig.6 to be LE1=-0.633<0 and LE2=-0.636<0. Again, synchronization occurs for a chaotic input signal whose Lyapunov exponents are LE1=0.0135>0, LE2=-0.0001432≈0 and LE3=-1.258<0. In case where there exists some discrepancy of parameters in two almost identical PLL's (PLL1 and PLL2) as in Figs. 4, 5, 7, and 8, some degradation of synchronization occurs, but this discrepancy does not diverge as time elapses. Therefore the two PLL's still have strong correlation. In contrast, for configuration 2, the Lyapunov exponents for the w sub-system have been calculated to be LE1=0.0846>0 and

$LE2=-0.646<0$ for the small-damping case in Fig.9, and $LE1=0.00083>0$ and $LE2=-1.277<0$ for the large-damping case in Fig.10. Indeed, synchronization of the two chaotic PLL's does not occur in this configuration even after a fine adjustment of their parameter values.

5. EXPERIMENTAL RESULT

In this section, we will present our experimental results for configuration 1 and configuration 2. Figure11 shows the actual experimental circuit of a PLL using an integrated circuit module MC14046B. Combining three or two such PLL's as in Fig.1 or Fig.2, respectively, we have built the experimental circuit for configuration 1 and configuration 2. The parameter values for r, R and C are chosen as $r=2.7$ kΩ, $R=51$ kΩ and $C=1000$ pF, thereby giving a loop filter time constant equal to $\tau=(R+r/2)\times C=52.4\times10^{-6}$. The total DC loop gain K_0 is determined from the lock range of $f_L=5.9$ kHz so that $K_0=2f_L=11.8\times10^3$ rad/sec. From these data, we have calculated the normalized natural frequency β and the damping coefficient ζ to be equal to $\beta=2\zeta=1/\sqrt{K_0\tau}=1.27$, which correspond to one of the parameters in our computer simulations for the large damping case. The natural frequency was calculated to be equal to $f_n=(1/2\pi)\sqrt{K_0/\tau}=2388$ Hz. Figure12 gives the experimental results for configuration 1, where Figs.12(a), (b), and (c) show the chaotic VCO spectrum of the PLL0, PLL1, and PLL2, respectively. Figure12(d) shows the voltage trace between the VCO outputs of the PLL1 and PLL2: the 45° straight line confirms that there is a complete synchronization. In Fig.12, all the VCO free-running frequencies are set equal to $f_{vco,0}=f_{vco,1}=f_{vco,2}=28$ kHz, and the carrier frequency and the modulation frequency of the input FM signal are set equal to $f_c=29.33$ kHz and $f_m=515$ Hz, respectively. Therefore, the normalized detuning is equal to $\sigma=(f_c-f_{vco,0})/f_n=0.432$ and the normalized modulation frequency is equal to $\Omega=f_m/f_n=0.215$. These parameter values are close to our computer simulation results shown in Fig.6, although σ is much smaller in this case. Figure13 is the result in which the free-running frequency of $f_{vco,2}$ is increased as $f_{vco,2}=30.88$ kHz while the other parameters remain the same as those in Fig.12. Hence, the VCO free-running frequencies of PLL1 and PLL2 have a detuning equal to $\delta=(3088-2800)/2388=0.12$. For this set of parameter values, the PLL1 and PLL2 can not be synchronized which corresponds to our computer simulation result of Fig.8(c).

Next, we present our experimental results for configuration 2 in Figs.14(a), (b) and (c). The experimental parameters are $f_{vco,1}=f_{vco,2}=26.8$ kHz, $f_c=30$ kHz and $f_m=473$ Hz. Figures 14(a) and (b) show the VCO spectra of the PLL1 and PLL2 are chaotic. Figure14(c) shows the trace of the VCO outputs of PLL1 and PLL2. In this configuration, the PLL1 and PLL2 have almost the same parameter values, yet synchronization is impossible to achieve. These experimental results are completely consistent with our *computer simulation* results.

6. CONCLUSIONS

We have shown that the chaotic VCO outputs of two identical PLL's which have a common chaotic input signal can synchronize with each other if the detuning of the VCO free-running frequencies is not large. We have also shown that the chaotic VCO outputs of two identical PLL's which have a common frequency modulated input signal with detuning can not be synchronized even after fine adjustments of the parameter values. By calculating the Lyapunov exponents of the respective sub-system, it is confirmed that they are all negative in configuration 1, but one of them is positive in configuration 2. Since PLL's are real systems widely used in the communication industry, synchronizing chaos in PLL's represents a first step towards the application of chaos in the design of *secure communication* systems.

References

[1] L.M. Pecora and T.L. Carrol, "Synchronization in chaotic systems", *Physical Review Letters*, Vol. 64, No.8, pp.821-824, Feb. 1990.

[2] T. L. Carrol and L.M. Pecora, "Synchronizing chaotic circuits", *IEEE Trans. Circuits Syst.*, Vol. CAS-38, No.4, pp.453-456, April 1991.

[3] Tetsuro Endo and Leon O. Chua, "Chaos from phase-locked loops", *IEEE Trans. Circuits Syst.*, vol. CAS-35, pp. 987-1003, Aug. 1988.

[4] Tetsuro Endo, Leon O. Chua and Tetsuya Narita, "Chaos from phase-locked loops, Part II: High-Dissipation Case", *IEEE Trans, Circuits Syst.*, vol. CAS-35, pp. 255-263, Feb. 1989.

[5] Tetsuro Endo and Leon O. Chua, "Bifurcation diagrams and fractal basin boundaries of phase-locked loop circuits", *IEEE Trans. Circuits Syst.*, vol. CAS-37, No.4, pp. 535-540, April 1990.

Figure captions:

Fig. 1: Phase-diagram of configuration 1

Fig.2: Phase-diagram of configuration 2

Fig.3: Synchronization of chaos in configuration 1 observed on a Poincare section for the small damping case: β=0.56, σ=1.43341, Ω=0.637, m=0.097. The loop-filter time constants are equal and the VCO free-running frequency has no detuning: κ_1=1, κ_2=1, δ=0. (a) chaotic attractor of the input signal (b) chaotic attractor in the PLL1 (c) trace between ϕ_1 and ϕ_2 representing complete synchronization (d) chaotic attractor in the PLL2

Fig.4: Synchronization of chaos in configuration 1 observed on a Poincare section for the small damping case: β=0.56, σ=1.43341, Ω=0.637, m=0.097. The loop-filter time constants are *not* equal and the VCO free-running frequency has no detuning: κ_1=1.05, κ_2=0.95, δ=0. (a) chaotic attractor of the input signal (b) chaotic attractor in the PLL1 (c) trace between ϕ_1 and ϕ_2 representing some correlation (partial synchronization) (d) chaotic attractor in the PLL2

Fig.5: Three traces between ϕ_1 and ϕ_2 for either unequal loop-filter time constants or non-zero detuning of the VCO free-running frequencies in configuration 1 for the small damping case: β=0.56, σ=1.43341, Ω=0.637, m=0.097. (a) κ_1=1.0, κ_2=1.0, δ=0.01 (b) κ_1=1.01, κ_2=0.99, δ=0.0 (c) κ_1=1.0, κ_2=1.0, δ=0.1

Fig.6: Synchronization of chaos in configuration 1 observed on a Poincare section for the large damping case: β=1.27, σ=1.15, Ω=0.2, m=0.053. The loop

filter time constants are equal and the VCO free-running frequency has no detuning: κ_1=1, κ_2=1, δ=0. (a) chaotic attractor of the input signal (b) chaotic attractor in the PLL1 (c) trace between ϕ_1 and ϕ_2 representing complete synchronization (d) chaotic attractor in the PLL2

Fig.7: Synchronization of chaos in configuration 1 observed on a Poincare section for the large damping case: β=1.27, σ=1.15, Ω=0.2, m=0.053. The loop-filter time constants are equal but the VCO free-running frequency has detuning: κ_1=1, κ_2=1, δ=0.05. (a) chaotic attractor of input signal (b) chaotic attractor in the PLL1 (c) trace between ϕ_1 and ϕ_2 representing partial synchronization (d) chaotic attractor in the PLL2

Fig.8: Three traces between ϕ_1 and ϕ_2 for either unequal loop-filter time constants or non-zero detuning of the VCO free-running frequencies in configuration 1 for the large damping case: β=1.27, σ=1.15, Ω=0.2, m=0.053. (a) κ_1=1.05, κ_2=0.95, δ=0.0 (b) κ_1=1.1, κ_2=0.9, δ=0.0 (c) κ_1=1.0, κ_2=1.0, δ=0.1

Fig.9: Non-synchronization of chaos in configuration 2 observed on a Poincare section for the small damping case: β=0.56, σ=1.43341, Ω=0.637, m=0.097. (a) chaotic attractor in the PLL1 (b) chaotic attractor in the PLL2 (c) trace between ϕ_1 and ϕ_2 showing no correlation with each other.

Fig.10: Non-synchronization of chaos in configuration 2 observed on a Poincare section for the large damping case: β=1.27, σ=1.15, Ω=0.2, m=0.053. (a) chaotic attractor in the PLL1 (b) chaotic attractor in the PLL2 (c) trace between ϕ_1 and ϕ_2 showing no correlation with each other.

Fig.11: Experimental circuit of a PLL using an integrated circuit module MC14046B.

Fig.12: Experimental verification of synchronization of chaos between the PLL1 and PLL2 in configuration 1. The PLL1 and PLL2 have almost identical parameter values.

Fig.13: Experimental demonstration of non-synchronized chaos in configuration 1. The PLL1 and PLL2 have almost identical parameter values. The VCO free-running frequencies have a detuning.

Fig.14: Experimental demonstration of non-synchronized chaos in configuration 2.

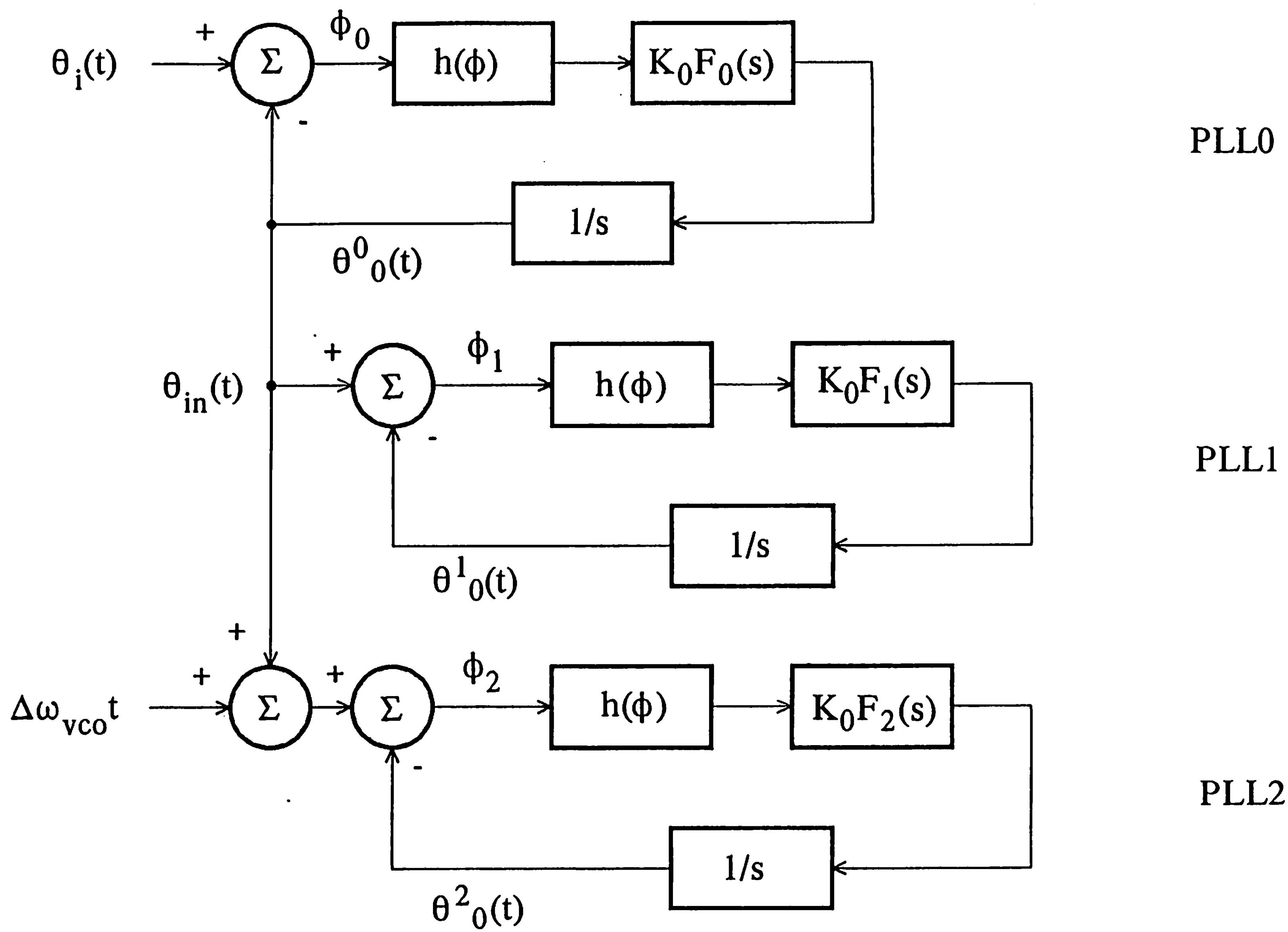

$\theta_i(t)$
+
Σ
-
ϕ_0
$h(\phi)$
$K_0F_0(s)$
$1/s$
$\theta^0{}_0(t)$
PLL0
$\theta_{in}(t)$
+
Σ
-
ϕ_1
$h(\phi)$
$K_0F_1(s)$
$1/s$
$\theta^1{}_0(t)$
PLL1
$\Delta\omega_{vco}t$
+
+
Σ
+
Σ
-
ϕ_2
$h(\phi)$
$K_0F_2(s)$
$1/s$
$\theta^2{}_0(t)$
PLL2

Fig. 1

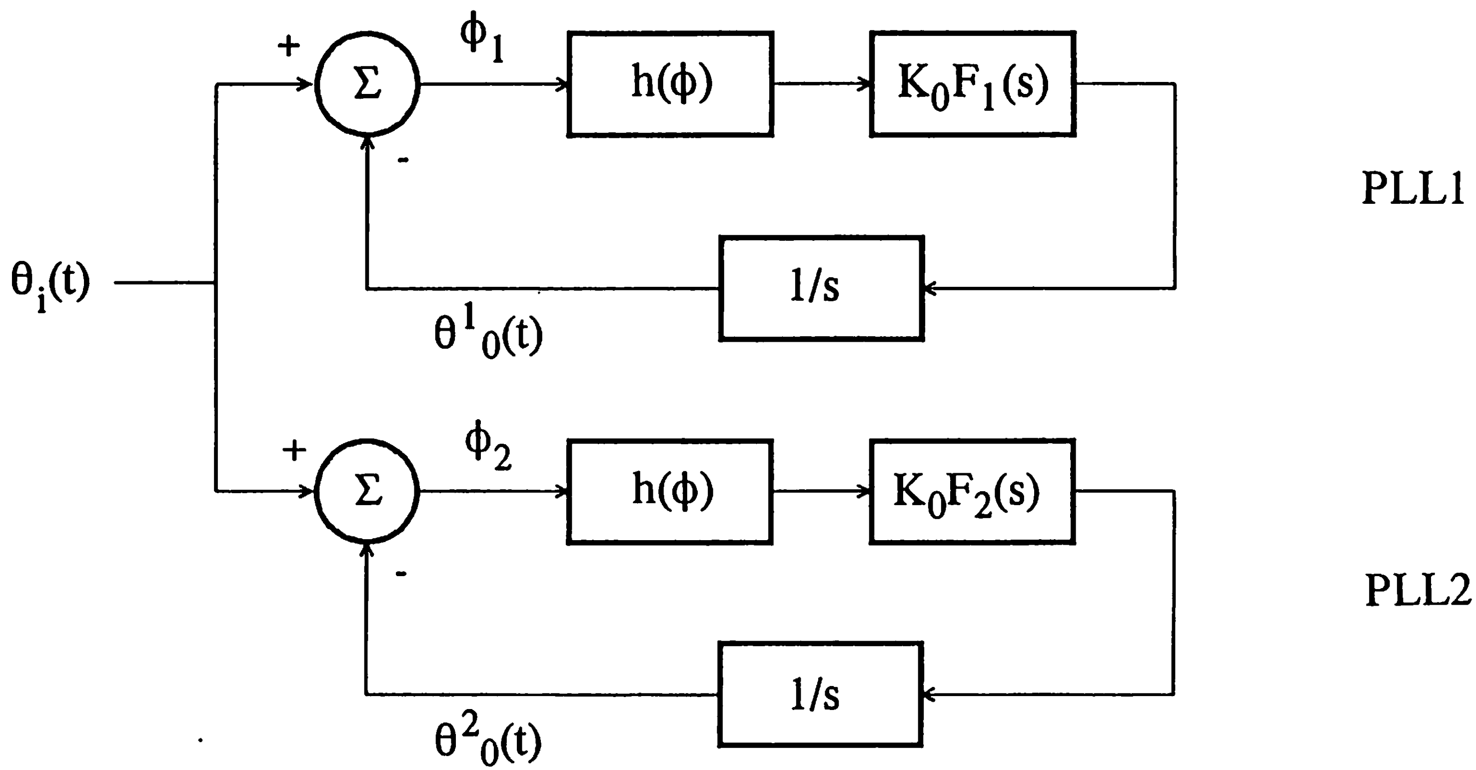

+
Σ
-
ϕ_1
h(ϕ)
$K_0F_1(s)$
PLL1
$\theta_i(t)$
1/s
$\theta^1{}_0(t)$
+
Σ
-
ϕ_2
h(ϕ)
$K_0F_2(s)$
PLL2
1/s
$\theta^2{}_0(t)$

Fig.2

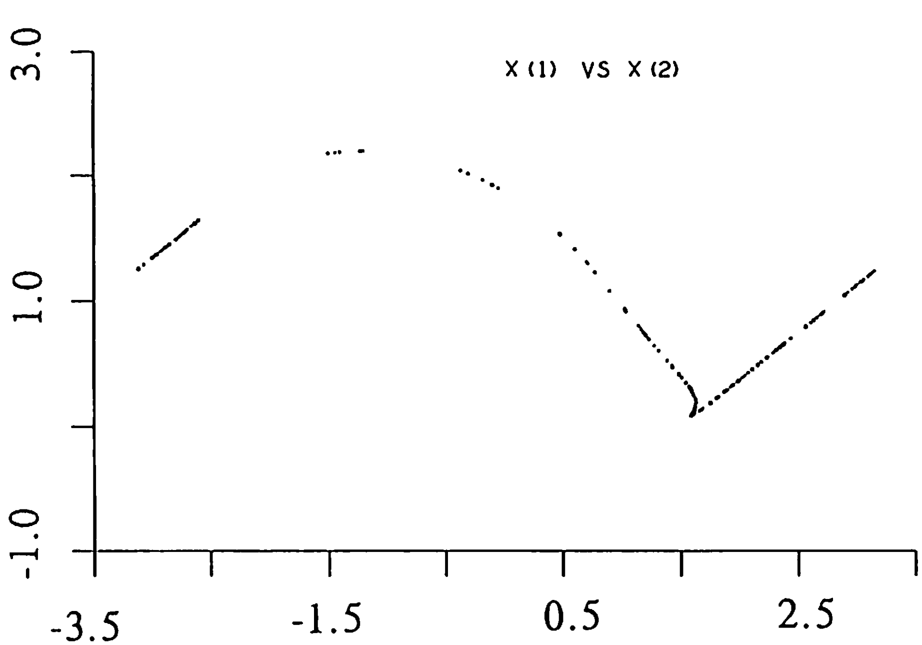

(a) X(1) vs X(2)

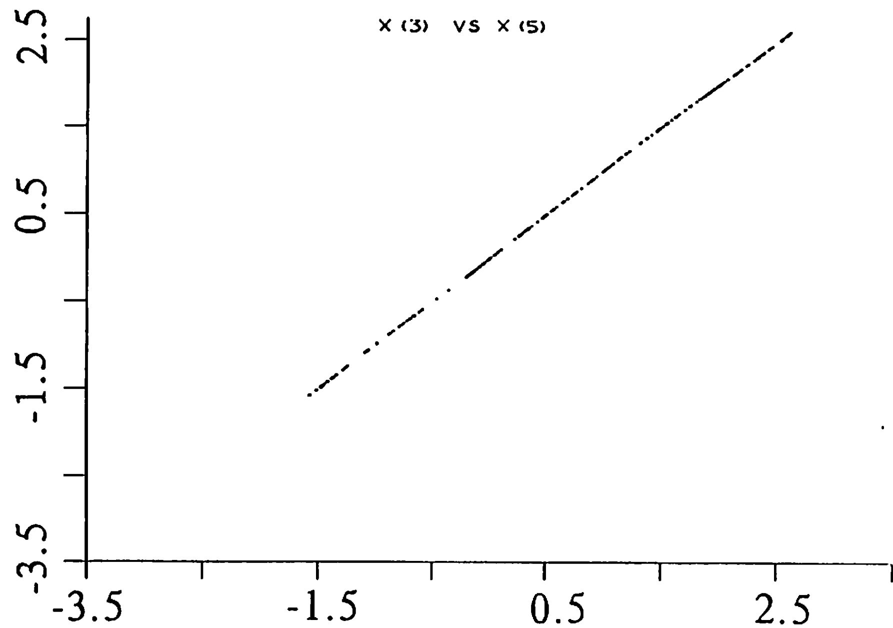

(c) X(3) vs X(5)

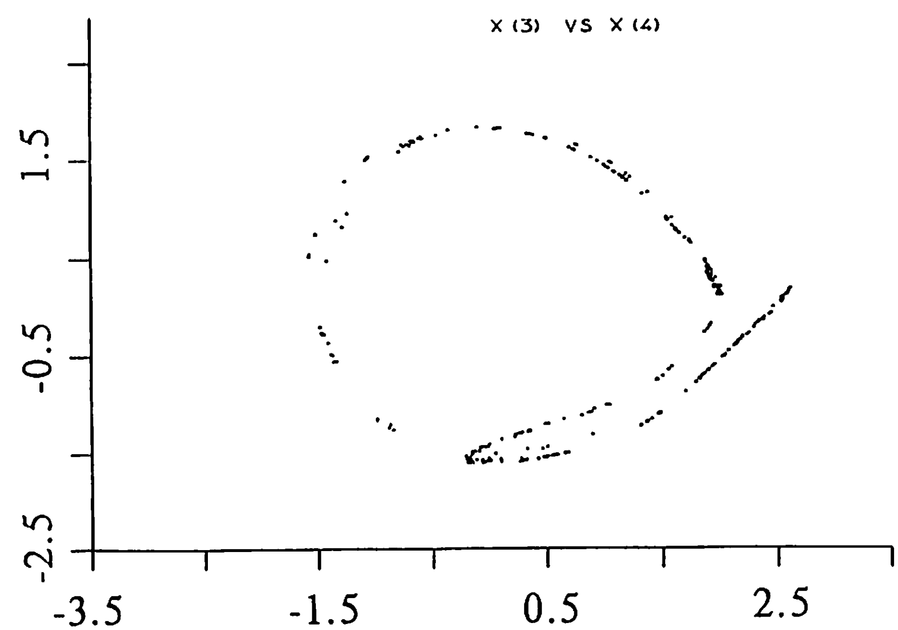

(b) X(3) vs X(4)

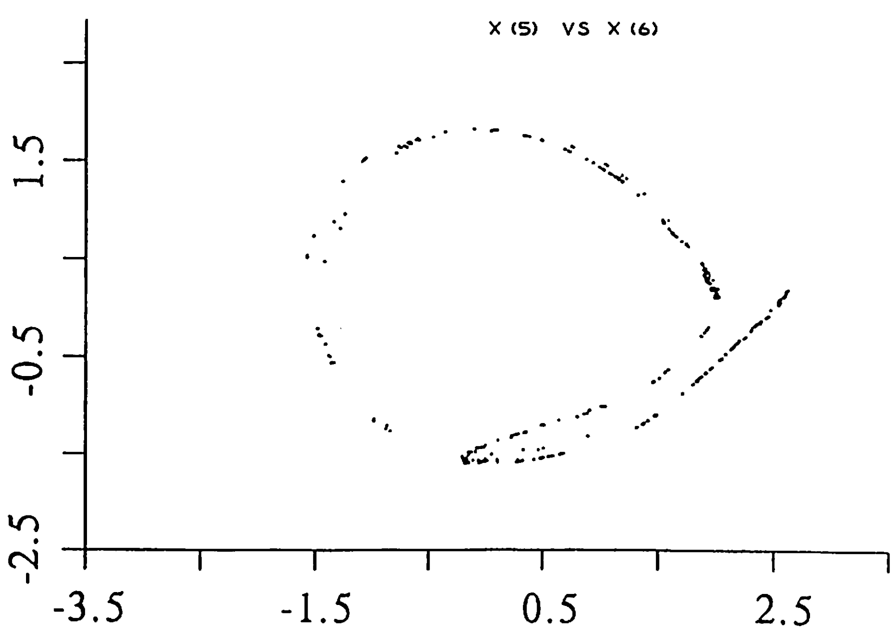

(d) X(5) vs X(6)

Fig.3

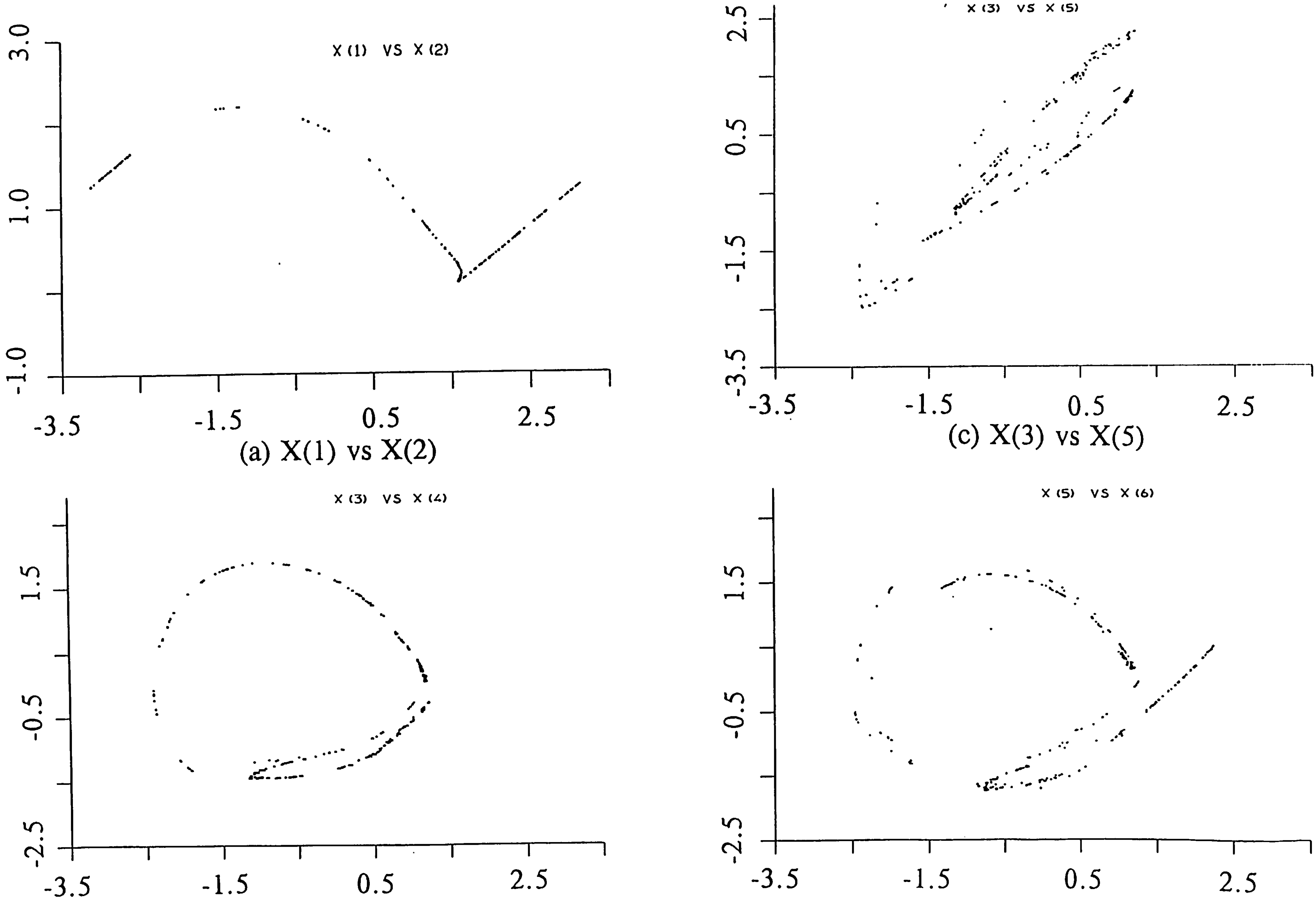

(a) X(1) vs X(2)

(c) X(3) vs X(5)

(b) X(3) vs X(4)

(d) X(5) vs X(6)

Fig.4

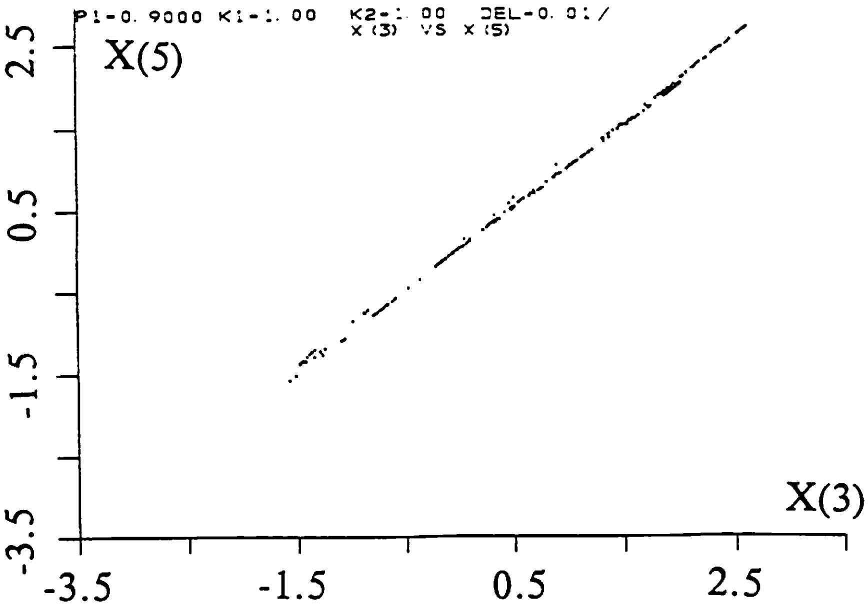

(a) $\kappa_1=1.0$, $\kappa_2=1.0$, $\delta=0.01$

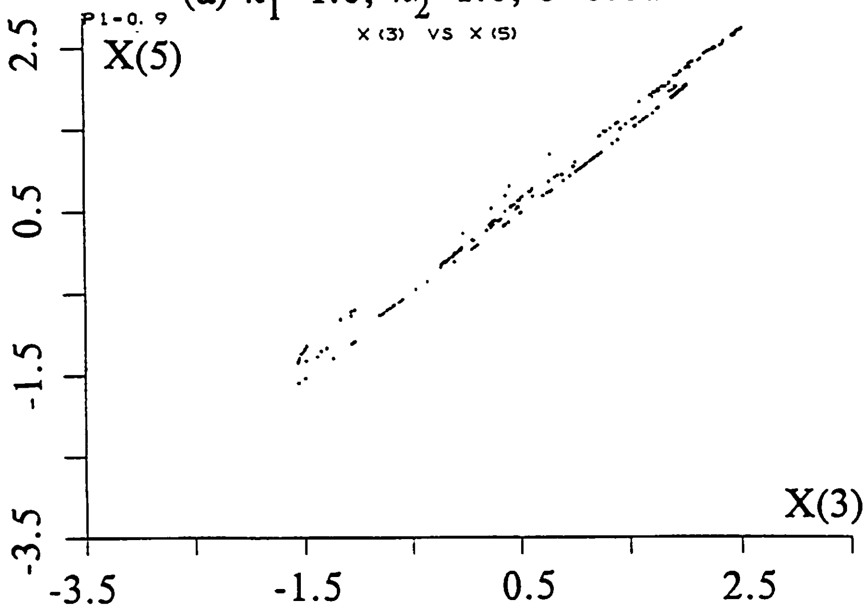

(b) $\kappa_1=1.01$, $\kappa_2=0.99$, $\delta=0.0$

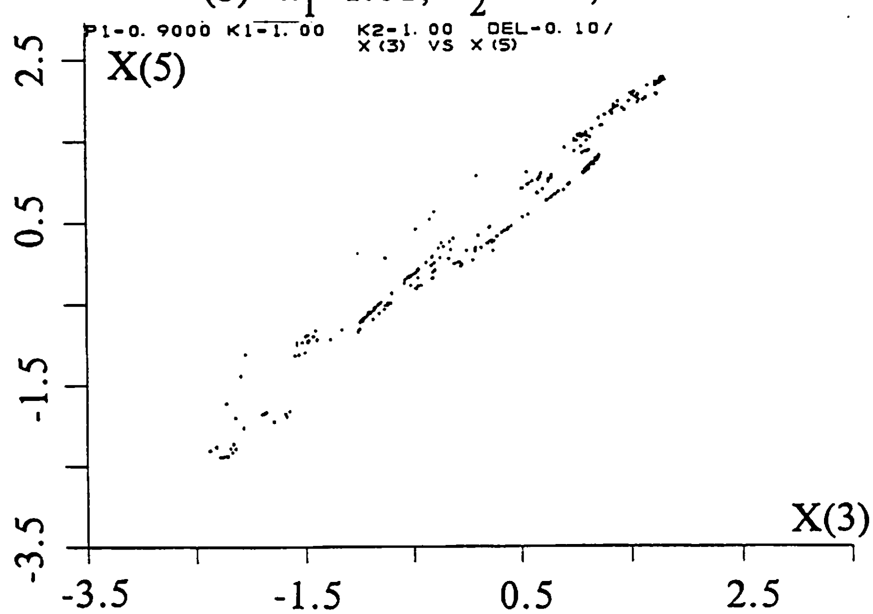

(c) $\kappa_1=1.0$, $\kappa_2=1.0$, $\delta=0.1$

Fig.5

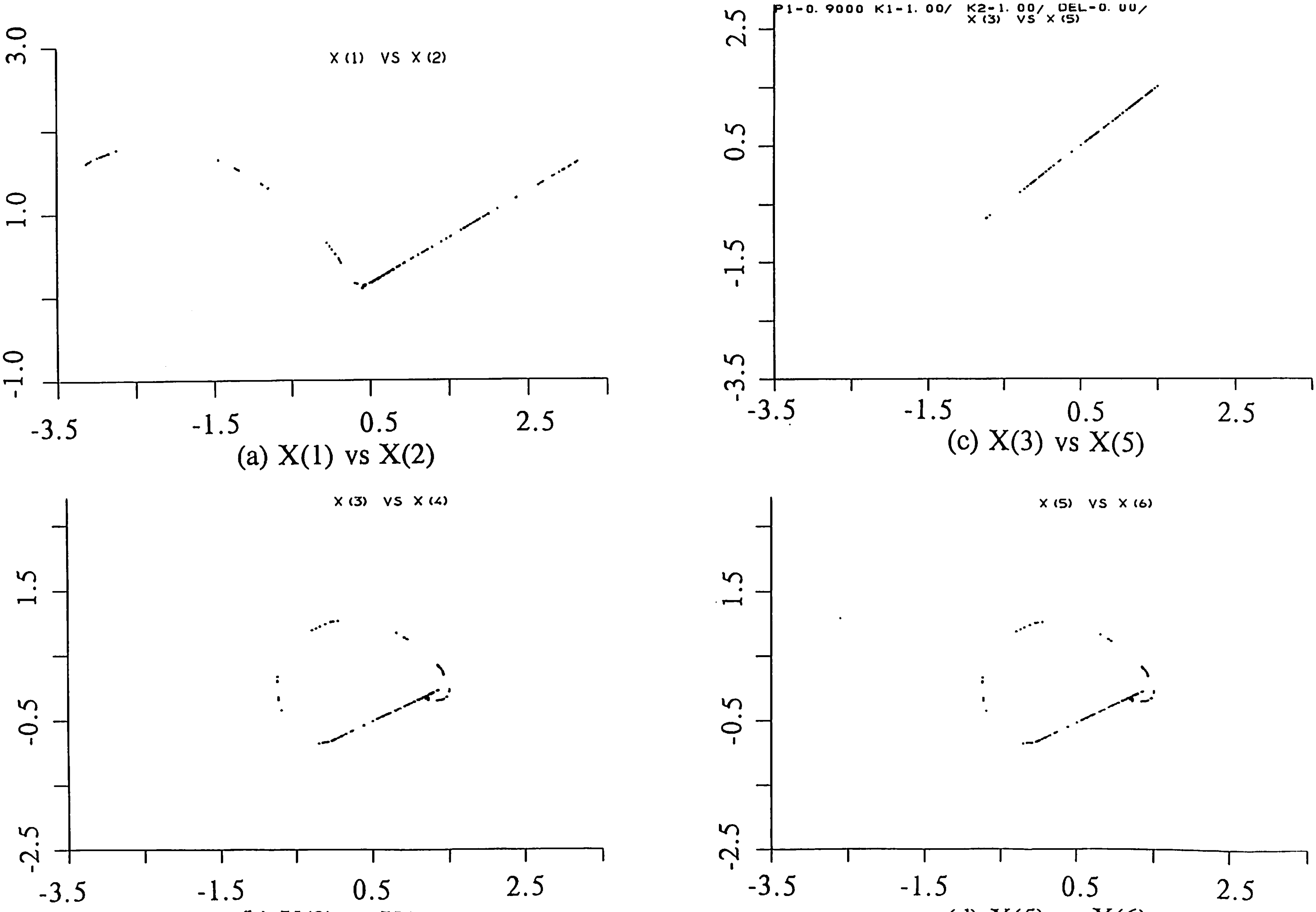

(a) X(1) vs X(2)

(b) X(3) vs X(4)

(c) X(3) vs X(5)

(d) X(5) vs X(6)

Fig.6

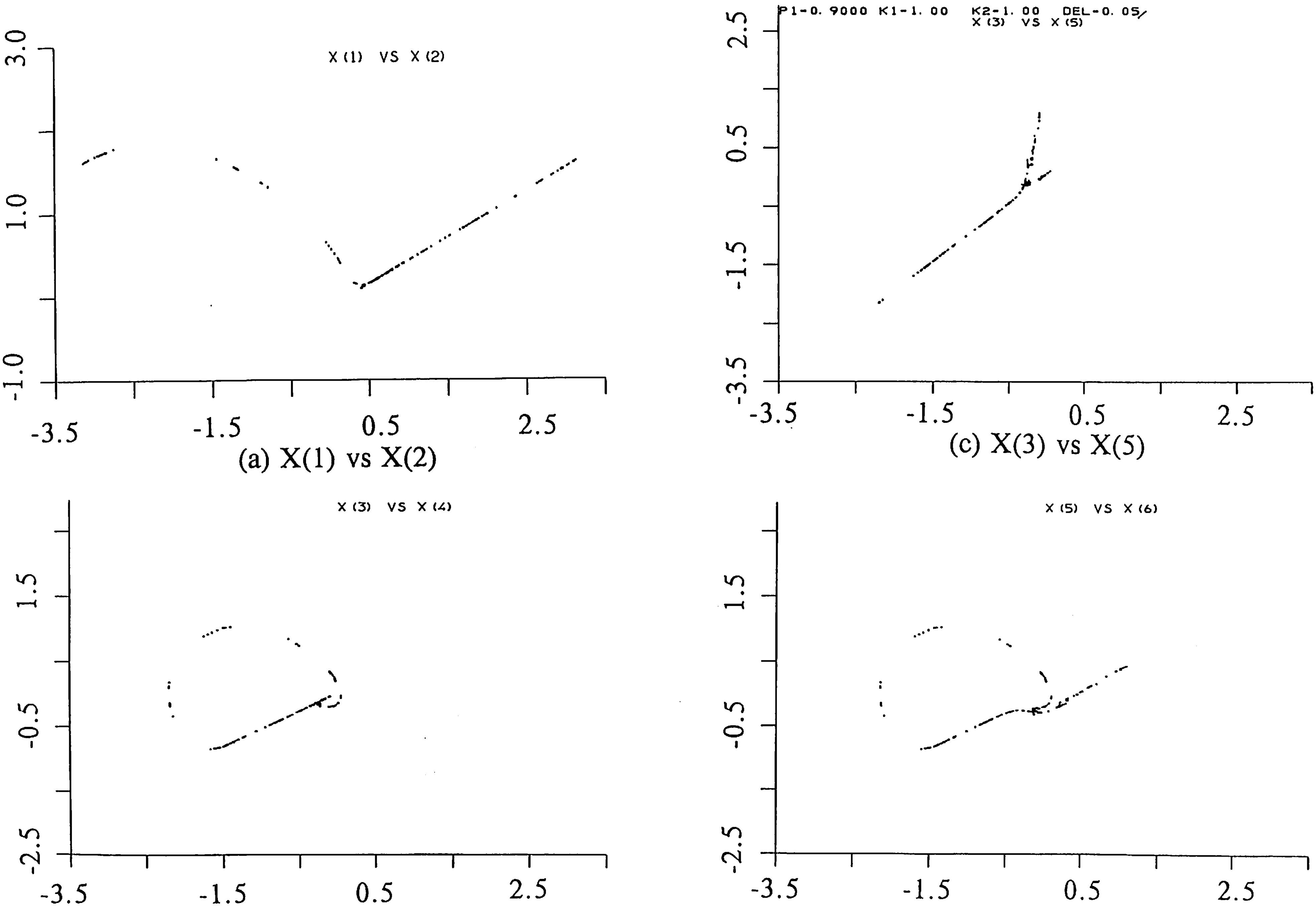

(a) X(1) vs X(2)

(c) X(3) vs X(5)

(b) X(3) vs X(4)

(d) X(5) vs X(6)

Fig.7

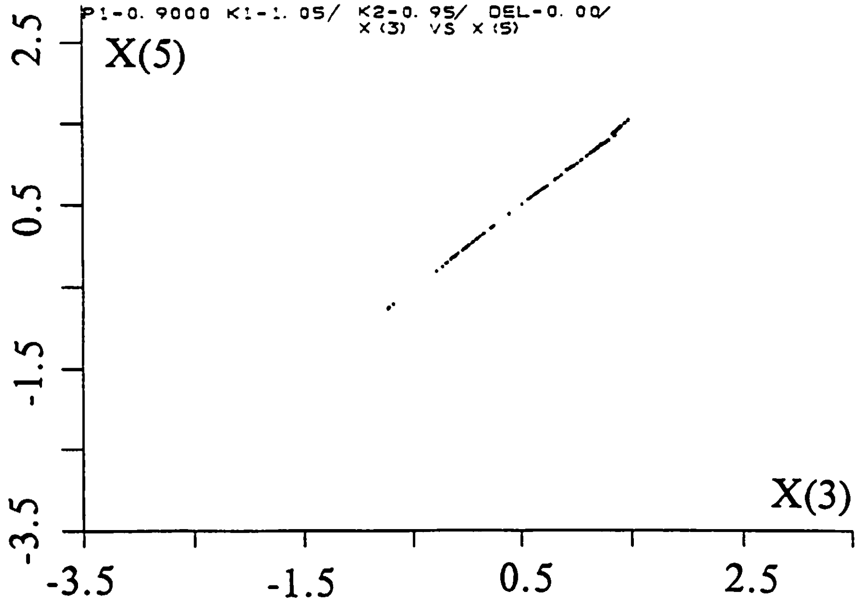

(a) κ_1=1.05, κ_2=0.95, δ=0.0

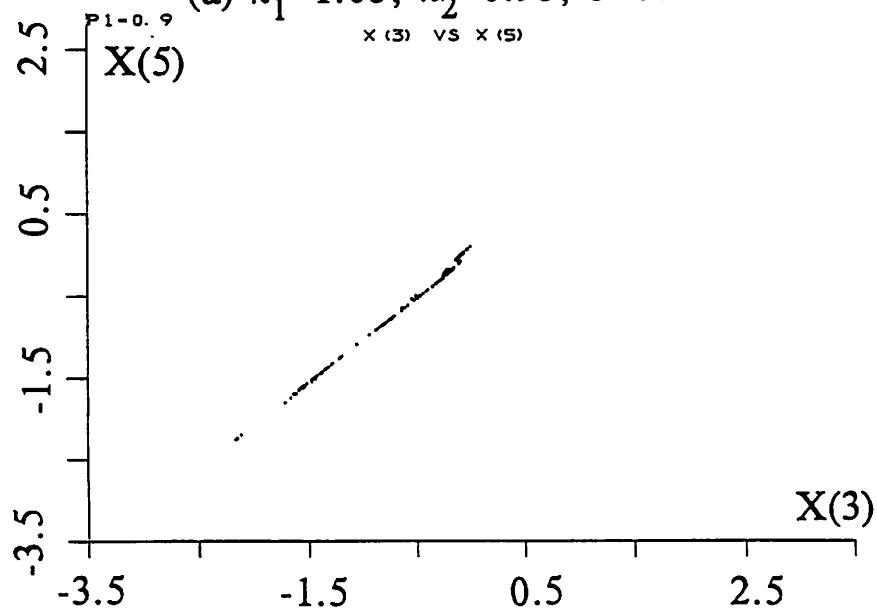

(b) κ_1=1.1, κ_2=0.9, δ=0.0

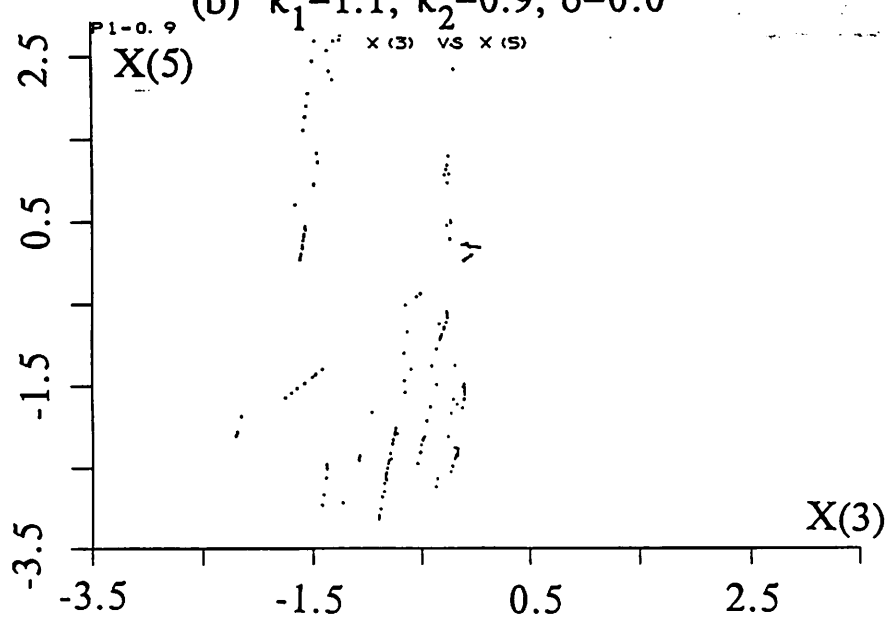

(c) κ_1=1.0, κ_2=1.0, δ=0.1

Fig.8

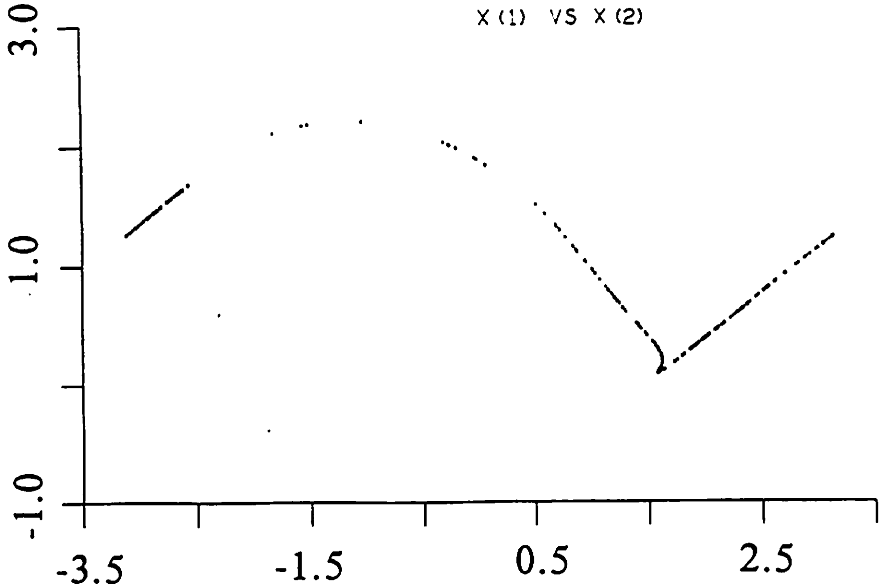

(a) X(1) vs X(2)

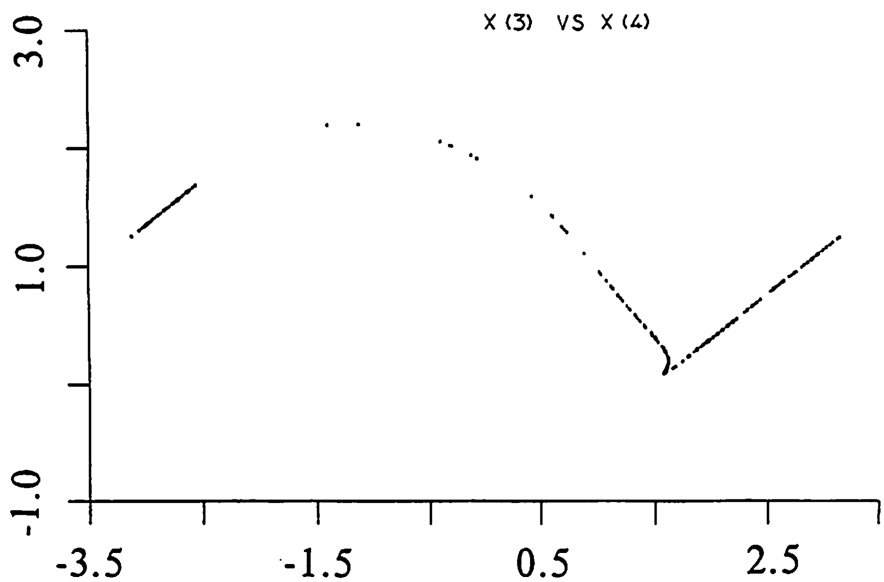

(b) X(3) vs X(4)

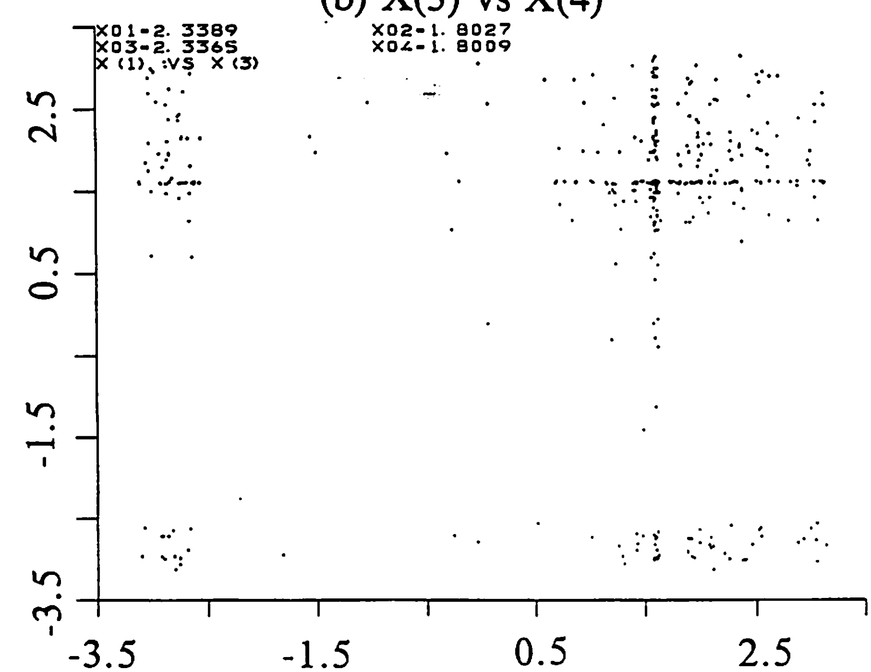

(c) X(1) vs X(3)

Fig.9

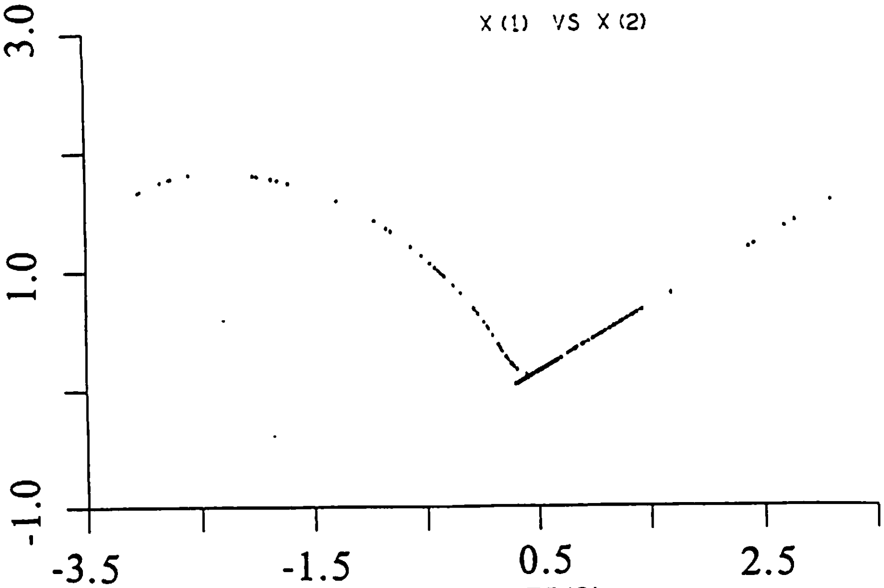

(a) X(1) vs X(2)

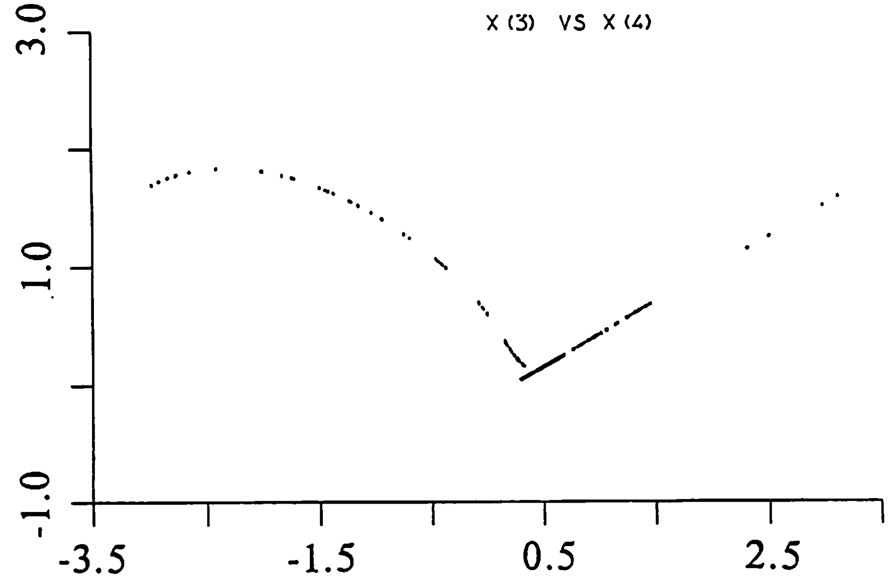

(b) X(3) vs X(4)

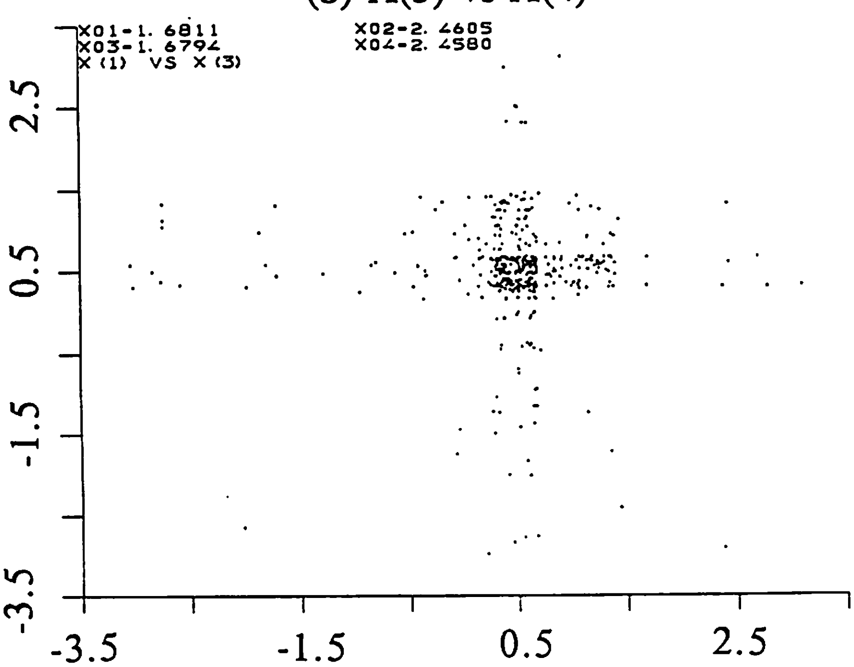

(c) X(1) vs X(3)

Fig.10

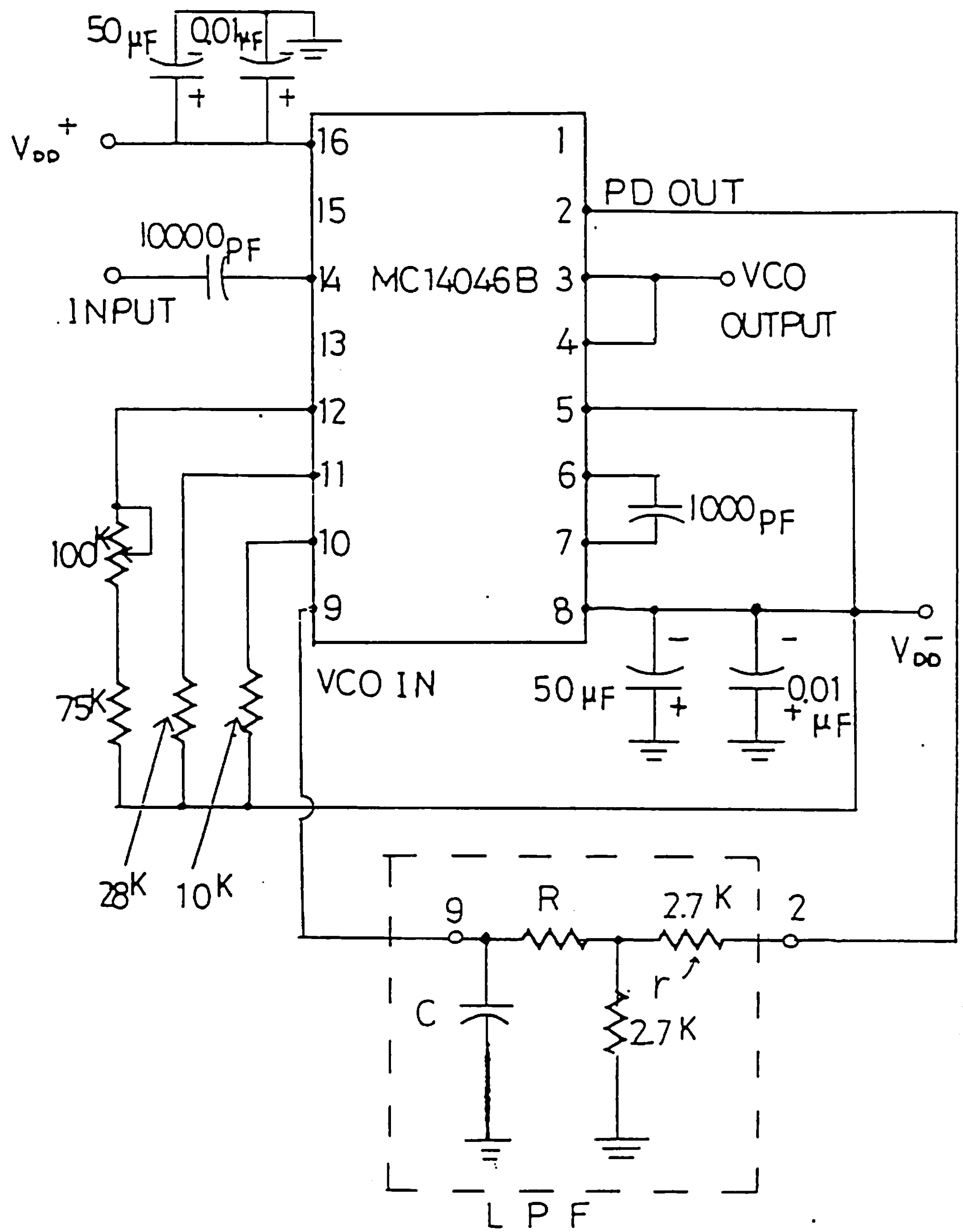

50μF
0.01μF
V_{DD}^{+}
16
1
15
2
PD OUT
10000PF
14
MC14046B
3
VCO
INPUT
OUTPUT
13
4
12
5
11
6
1000PF
100K
10
7
9
8
V_{DD}^{-}
VCO IN
50μF
0.01μF
75K
28K
10K
9
R
2.7K
2
r
C
2.7K
L P F

Fig.11

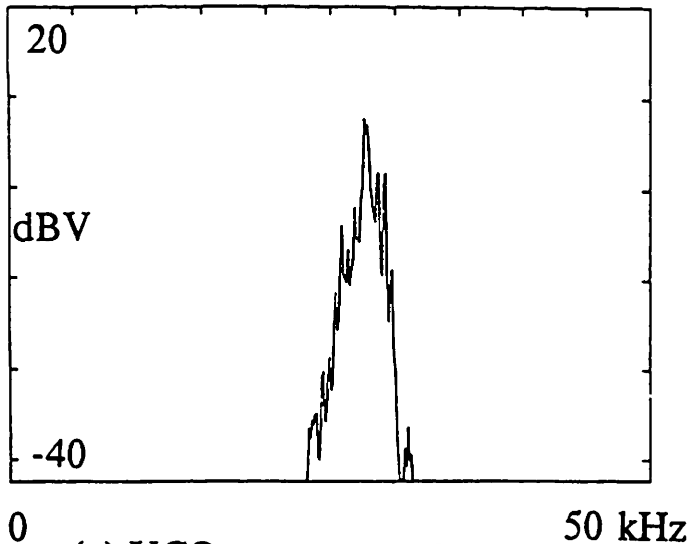

(a) VCO spectrum of PLL0

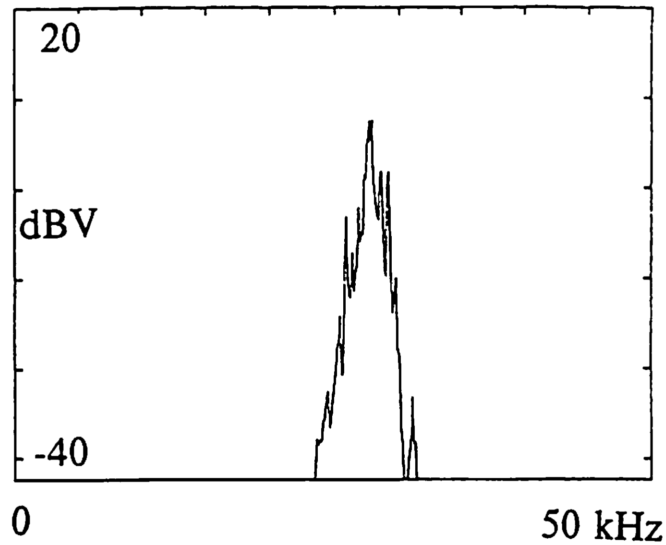

(c) VCO spectrum of PLL2

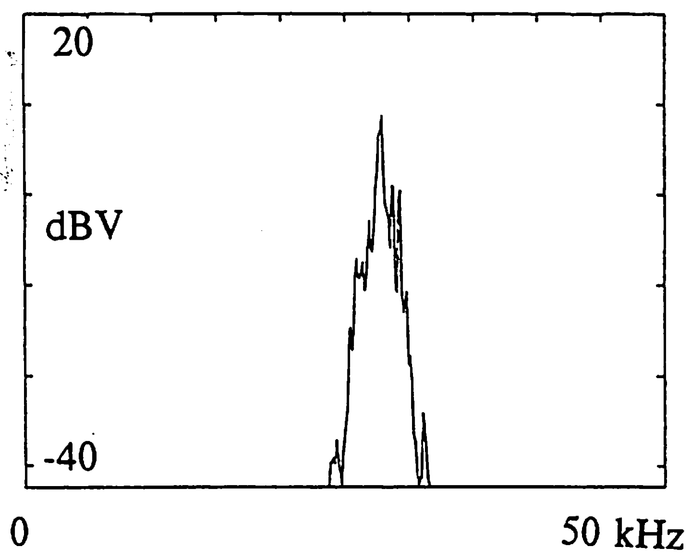

(b) VCO spectrum of PLL1

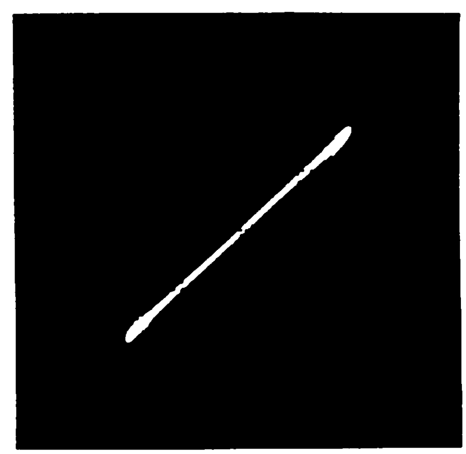

(d) VCO voltage trace between PLL1 and PLL2

Fig. 12

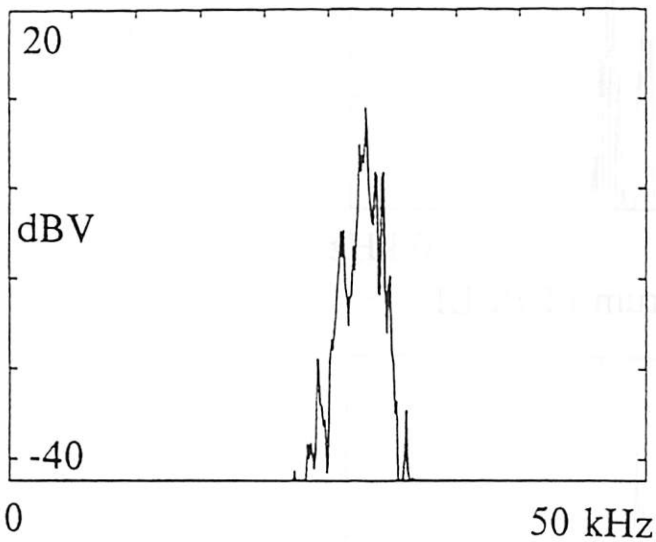

(a) VCO spectrum of PLL0

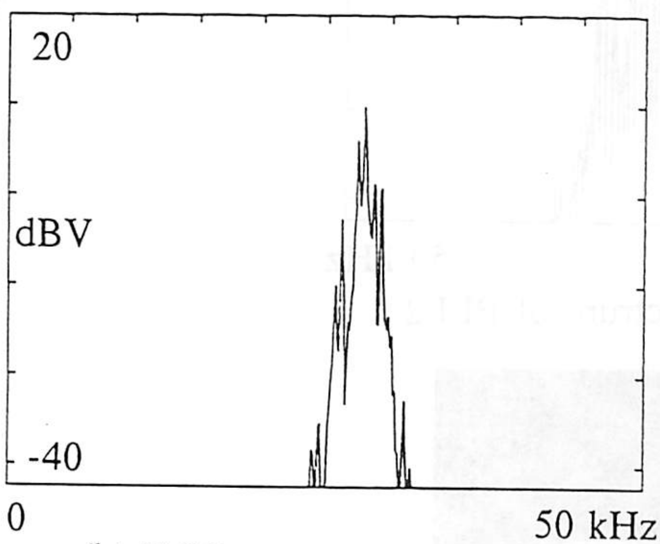

(b) VCO spectrum of PLL1

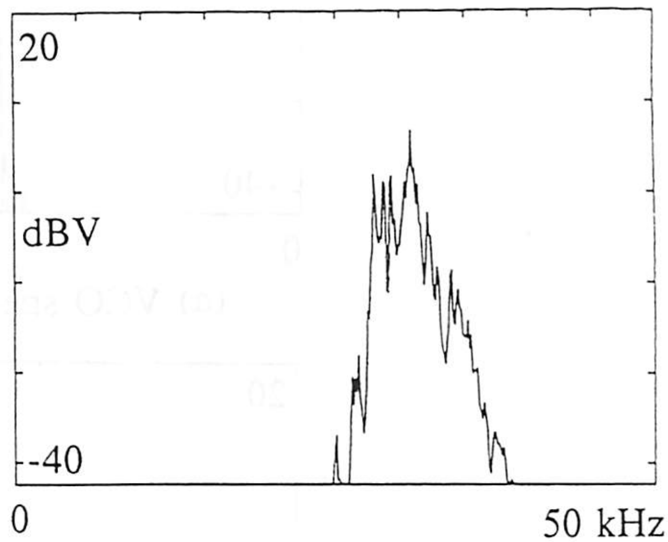

(c) VCO spectrum of PLL2

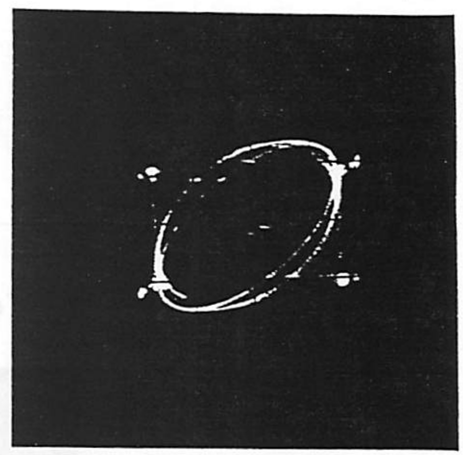

(d) VCO voltage trace between PLL1 and PLL2

Fig.13

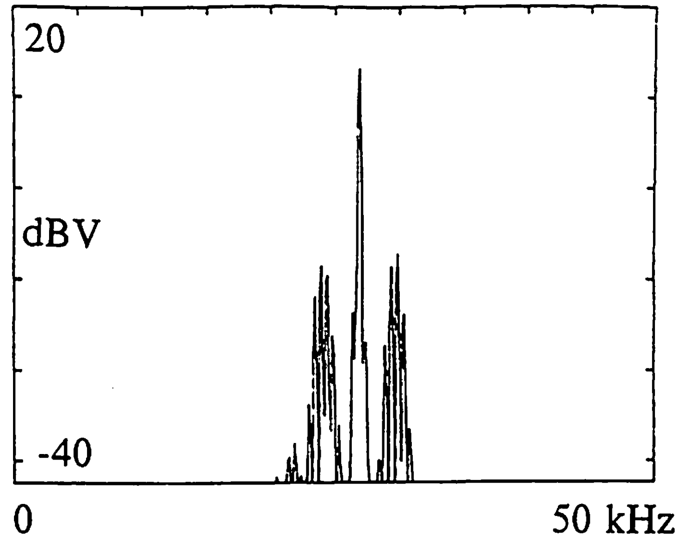

(a) VCO spectrum of PLL1

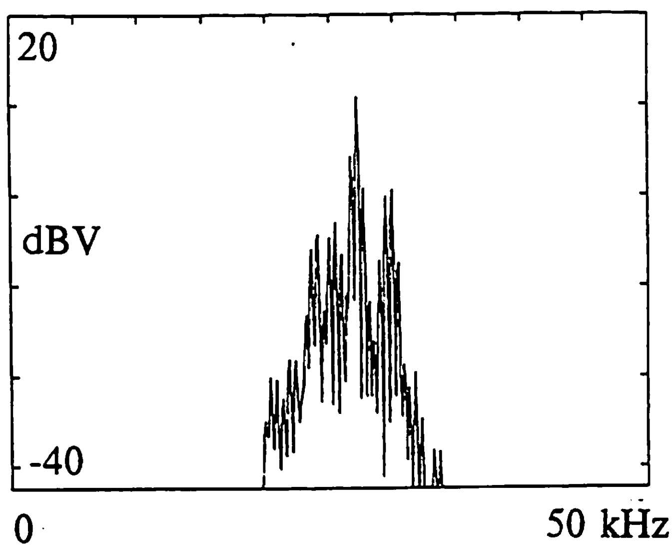

(b) VCO spectrum of PLL2

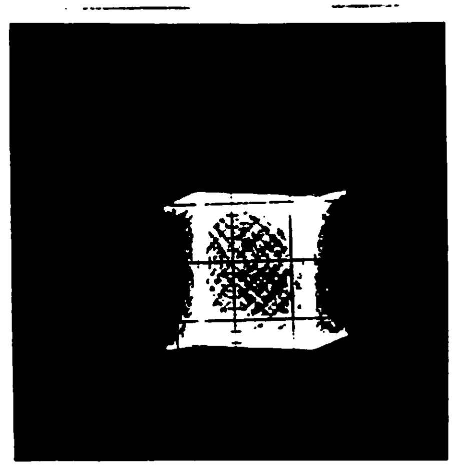

(c) VCO voltage trace between PLL1 and PLL2

Fig.14